This is the peer reviewed version of the following article:

Cabrera-González J., Cabana L., Ballesteros B., Tobias G., Núñez R.. Highly Dispersible and Stable Anionic Boron Cluster-Graphene Oxide Nanohybrids. Chemistry - A European Journal, (2016). 22. : 5096 - . 10.1002/chem.201505044,

which has been published in final form at https://dx.doi.org/10.1002/chem.201505044. This article may be used for non-commercial purposes in accordance with Wiley Terms and Conditions for Use of Self-Archived Versions.

Highly dispersible and stable anionic boron clusters-graphene oxide nanohybrids.

Justo Cabrera-González,[a] Laura Cabana,[a] Belén Ballesteros,[b] Gerard Tobias,*[a] and Rosario Núñez*[a]

[a] J. Cabrera-González,† Dr. L. Cabana, Dr. G. Tobias, Dr. R. Núñez
Institut de Ciència de Materials de Barcelona (ICMAB-CSIC), Campus UAB 08193 Bellaterra, Barcelona (Spain)
E-mail: rosario@icmab.es ; gerard.tobias@icmab.es

[b] Dr. B. Ballesteros
Catalan Institute of Nanoscience and Nanotechnology (ICN2) , CSIC and The Barcelona Institute of Science and Technology
Campus UAB 08193 Bellaterra, Barcelona (Spain)

† J.C.-G. is enrolled in the UAB Ph.D. program.

Abstract: An efficient process to produce boron clusters-graphene oxide nanohybrids that are highly dispersible in water and organic solvents is established for the first time. Dispersions of these nanohybrid materials in water were extraordinarily stable after one month. Characterization of hybrids after grafting of appropriate cobaltabisdicarbollide and *closo*-dodecaborate derivatives onto the surface of graphene oxide (GO) was done by FT-IR, XPS and UV-vis. Thermogravimetric analysis (TGA) clearly shows a higher thermal stability for the modified–GO nanohybrids compared to the parent GO. Noteworthy, elemental mapping by EFTEM reveals that a uniform decoration of the graphene oxide surface with the boron clusters is achieved under the reported conditions. Therefore, the resulting nanohybrid systems show exceptional physico-chemical and thermal properties, paving the way for an enhanced processability and further expanding the range of application for graphene based materials.

In the last decade, graphene has been making a profound impact in many areas of science and technology due to its exceptional and unique chemical and physical properties.[1] The strong van der Waals interactions between graphene sheets lead to aggregation and poor solution processability, being a major drawback for many of the envisaged applications. To overcome these limitations, chemical modification of the graphitic structure has been widely employed. One of the most conventional methods consists on the treatment of graphite with strong oxidizing acids thus leading to the formation of graphene oxide (GO)[2]. The presence of oxygen-containing functional groups not only renders graphene water dispersible but also raises as a an excellent starting point for further derivatisation chemistry.[3] The formation of these carbon-based hybrid materials is an efficient way not only to exploit the synergies of both constituent elements but it can also lead to unique properties,[4] which open the way to applications in nanodevices[5] and biomedicine,[6] among others.

On the other hand, the recent advances in the preparation of boron cluster-based materials for nanotechnology and drug design have greatly expanded their potential use in these fields.[7] From the large group of boron cluster compounds, the cobaltabisdicarbollide anion (or cosane), $[3,3'\text{-}Co(C_2B_9H_{11})_2]^-$, and the dodecahydro-*closo*-dodecaborate, also referred to as *closo*-dodecaborate dianion $[B_{12}H_{12}]^{2-}$, are receiving an increased interest. The $[3,3'\text{-}Co(C_2B_9H_{11})_2]^-$ has exceptional chemical and thermal stability, as well as uncommon physico-chemical properties in water due to the self-assembling capacity,[8] inducing the ability to assemble into micelles and monolayer vesicles.[9] This anion can be accumulated *in vitro* within living cells[10] and after radiolabelling the cosane with ^{125}I and ^{124}I, it can be visualized *in vivo* by PET-CT.[11] Moreover, the $[B_{12}H_{12}]^{2-}$ shows high chemical and hydrolytic stability, high solubility in water as sodium salt, a better surfactant behaviour than the cosane[12] and low toxicity that are significant features for the design of pharmaceuticals, making this anion and its derivatives ideal candidates for cancer treatment with boron neutron capture therapy

(BNCT).[13] Additionally, the $[B_{12}H_{12}]^{2-}$ finds application as molecular motors and actuators capable of delivering useful work to nano-devices for photochemical or electrochemical power sources.[14] Despite their exceptional properties, the functionalization of surfaces with cosane,[15] and $[B_{12}H_{12}]^{2-}$ anions has been scarcely explored. Due to the uniqueness of these boron cluster anions, we are convinced that the modification of GO with them is of crucial importance to develop new materials for medical applications and devices.

Here we report an easy and efficient covalent functionalization of GO with the appropriate amine derivatives of *closo*-dodecaborate and cosane anions. The attachment of these boron clusters has been corroborated by FT-IR, UV-Vis, XPS, and TGA analysis. Although neutral boron cluster detection by EELS was established,[16] herein an anionic boron cluster was detected and mapping by EFTEM for the first time. Furthermore, we report here the first example of the covalent attachment of *closo*-dodecaborate on a surface.

Starting from boron clusters $[3,3'\text{-}Co(8\text{-}C_4H_8O_2\text{-}1,2\text{-}C_2B_9H_{10})(1',2'\text{-}C_2B_9H_{11})]$ (**1**) and $[B_{12}H_{11}(C_4H_8O_2)]^-$ (**2**) (see Scheme 1a), their respective derivatives, $[8\text{-}NH_2\text{-}C_4H_8O_2\text{-}3,3'\text{-}Co(1,2\text{-}C_2B_9H_{10})(1',2'\text{-}C_2B_9H_{11})]^-$ (**3**) and $[1\text{-}(8\text{-}NH_2\text{-}C_4H_8O_2)\text{-}B_{12}H_{11}]^{2-}$ (**4**), were obtained by using the procedure earlier described.[15b, 17] GO was prepared by a modified Hummer's method from graphite powder.[18] The boron clusters were covalently grafted onto the graphene oxide sheets via an amide and amine formation between **3** and **4** and oxygen-containing groups (e.g., carboxyl groups and epoxy) of GO.[3b] The functionalization reaction was performed by adding N,N-dicyclohexylcarbodimide (DCC) and 1-hydroxybenzotriazole (HOBt) to a dispersion of GO in dry N,N-dimethylformamide (DMF). This mixture was stirred for 30 min followed by the addition of **3** or **4**. The reaction was performed at 40˚C during 72h, to give **Cosane-GO** and **B$_{12}$-GO** hybrids, respectively (Scheme 1b).

Scheme 1. (a) Starting oxonium-derivative boron clusters. (b) Chemical functionalization of GO with anionic boron clusters

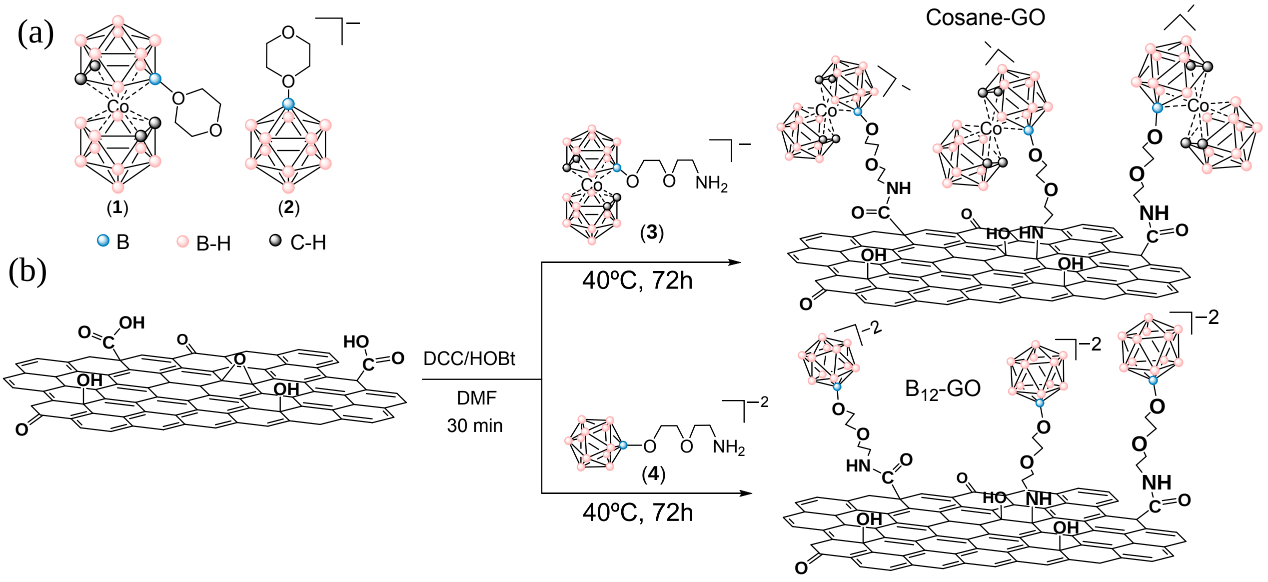

Characterization of the hybrid materials by FT-IR spectroscopy points out structural changes after functionalization of the GO (Figure 1). For **B_{12}-GO** and **Cosane-GO** hybrids the ν(B–H) vibration band appears at around 2487 and 2541 cm$^{-1,}$ respectively, which is in a similar range to a previously described neutral carborane cluster-GO hybrid.[19] After the grafting reaction, relative changes of the C=O stretching band (from carboxylic groups at 1730 cm^{-1}) and the C-O band (from epoxy groups at 1226 cm^{-1}), with respect to the C=C stretching band (1580 cm^{-1}) are detected.[19,20] Additionally, a shoulder at ~1650 cm^{-1} from the stretching ν(NC=O) vibration is observed[21] for **B_{12}-GO** and **Cosane-GO** hybrids.

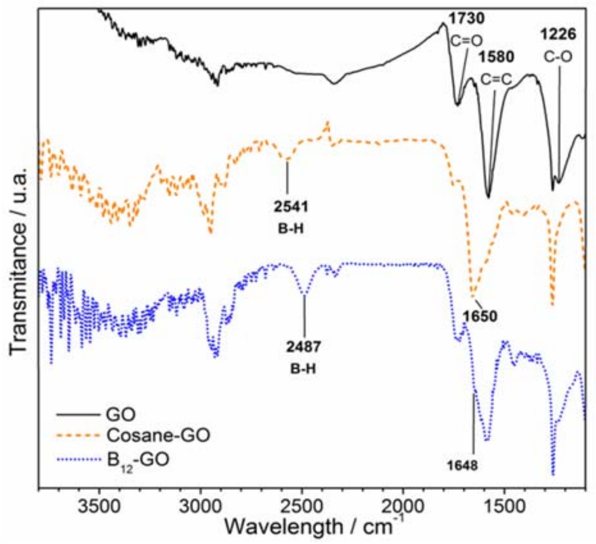

Figure 1. Infrared spectra of starting GO and modified-GO materials.

The modification of the GO surface by boron clusters was also quantitatively determined by conducting thermogravimetric analysis (TGA) in air (Figures S1-S3). GO presents a remarkable weight loss at 220 ˚C due to the elimination of oxygen bearing functionalities and the sample is completely combusted at about 600 ˚C. For **B_{12}-GO** and **Cosane-GO** the complete oxidation of the hybrid takes place at higher temperatures, between 600 and 720 ˚C, due to the presence of highly thermally stable borane clusters.[22] The degree of functionalization can be determined from the residue after the complete combustion of the different samples. During the process all the carbon from the GO and the organic part from the boron cluster compounds get oxidized. Hence, the solid residue obtained comes from inorganic materials and the oxidized boron cluster compounds. As expected, the residual mass after the complete combustion at 900 ˚C is higher for both **B_{12}-GO** and **Cosane-GO** compared to GO (see SI). Therefore we can establish that **Cosane-GO** and **B_{12}-GO** hybrids contain around 20.8 wt. % and 18.3 wt. % of the respective boron cluster derivatives. This indicates that the degree of functionalization of the GO with **3** and **4** is 484 µmol/g for **Cosane-GO** and 375 µmol/g for **B_{12}-GO**. Considering that the main components of the hybrids are carbon and the boron clusters, this degree of functionalization would correspond to one *closo*-dodecaborate cluster every 187 C atoms for **B_{12}-GO** and one cosane cluster every 136 C atoms for **Cosane-GO**. These levels of functionalization are similar to the recent report on the functionalization of graphene with carborane.[23] As a result, the presence of boron clusters covalently grafted to the graphene oxide surface causes an enhancement of the thermal stability of the nanohybrid materials.

X-ray Photoelectron Spectroscopy (XPS) analysis directly confirm the covalent bonding of **3** and **4** onto GO. For **Cosane-GO** hybrid, B and Co can be detected in the general survey scan as well as in the high resolution XPS over the B 1s and Co 2p regions (Figures S4). Moreover, the ratio between the two elements was determined to be 21:1, in agreement with the stoichiometry of the cosane used for the synthesis. On the other hand, for **B_{12}-GO** boron was detected in the general survey scan and high resolution XPS (Figure S5). High resolution of the C 1s region clearly reveals the chemical modification of GO with boron cluster compounds. By doing the deconvolution, we can observe the different functionalities present on the structure of GO (Figure 2a). For **B_{12}-GO** (Figure 2b) and **Cosane-GO** (Figure 2c) hybrids, the intensities of C-O/C-O-C, at 285.8 and 285.5 eV respectively, have dramatically decreased, as well as the C=O signal from starting GO at 288.6 eV. Moreover a new deconvolution curve attributed to C-N appears from 286.0 to 286.4.[24] This further confirms the covalent functionalization of the GO with the chosen boron clusters.

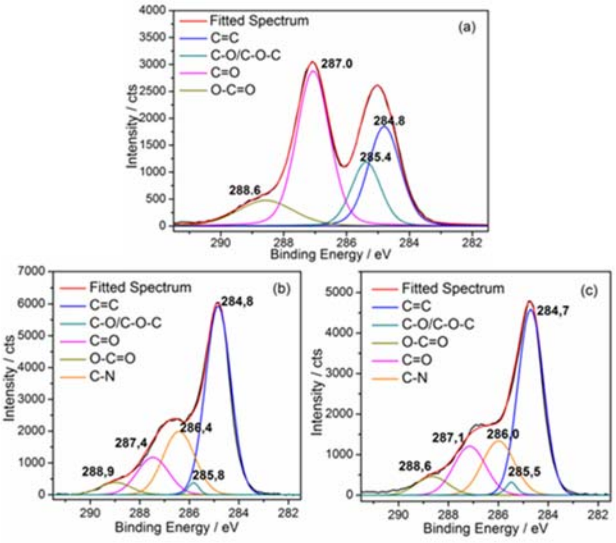

Figure 2. High resolution XPS spectra in the C 1s region for (a) GO, (b) **B_{12}-GO** and (c) **Cosane-GO** Figure Caption.

Moreover, the selected area electron diffraction (SAED) pattern of **B_{12}-GO** shows well defined diffraction spots that correspond to the crystalline structure of the graphene (Figure S7). In this SAED pattern of **B_{12}-GO** is no longer possible to observe the crystalline structure of compound **4** (Figure S6), confirming the attachment of the boron cluster as individual entities onto the surface of GO.

In regard to **Cosane-GO**, STEM-EDX was used to identify the cobalt atoms from cosane clusters. The signals at 6.924 and 0.776 keV, which belong to the energy dispersive X-ray signal from cobalt, certify the presence of **3**, hence the functionalization of GO (Figure S8).

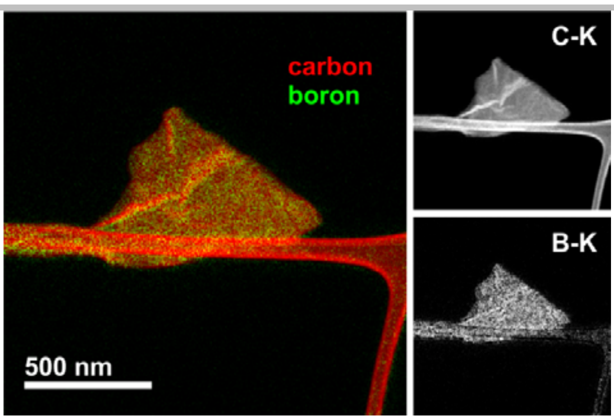

Figure 3. EFTEM elemental distribution maps of carbon and boron on sample **B_{12}-GO**.

In the case of **B_{12}-GO** STEM-EDX was not useful to confirm the success of the functionalization as detection of light elements (such as B or C) presents a challenge for EDX. Instead EELS and energy filtered transmission electron microscopy (EFTEM) were used. EELS analysis on a graphene flake shows the B-K and C-K edges, together with the O-K and N-K also present in the sample (Figure S9). The corresponding EFTEM elemental distribution maps taken on the K-ionization edges of B and C are shown in Figure 3. Carbon is found both on the graphene flake and the carbon support film, whereas the boron map only shows bright intensity on the graphene flake (see Figures S10 and S11 for additional EFTEM maps).

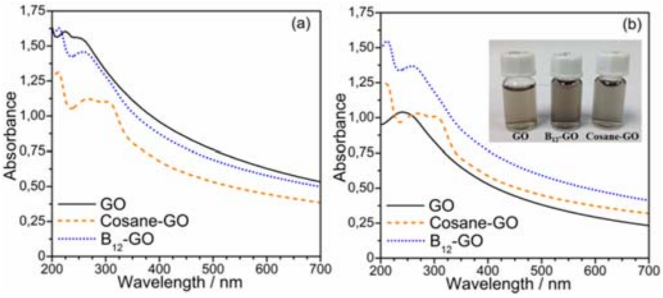

Figure 4. UV-Vis absorption spectra of GO, **Cosane-GO** and **B_{12}-GO** dispersed in water (a) as-prepared and (b) after 1 month.

UV-Vis spectra were next acquired to assess the dispersibility of GO and GO functionalized with cosane and *closo*-dodecaborate anions in H_2O. The resulting spectra of as-prepared dispersions in water for the tree samples (1 mg/mL) are exhibited in Figure 4a. The functionalized samples were compared with GO since it is well known that this material presents a high dispersibility in water.[3a] The UV-Vis spectrum of GO shows a characteristic maximum absorption peak at around 240 nm attributed to the π-π^* transition of aromatic C-C bonds.[25] In the modified-GO hybrids with anionic boron clusters, this absorption band is red-shifted about 15-30 nm when the supernatant liquid is analysed, which confirms the chemical modification of GO.[25-26] In the **Cosane-GO** dispersions the band around 305 nm is characteristic from the cosane anion.[27] The absorbance at $\lambda = 240$ nm was employed to assess the relative degree of dispersion. For ease of comparison, the absorbance of GO at 240 nm was set as 100 %. The as-prepared dispersions of GO and **B_{12}-GO** present a similar degree of dispersibility, whereas **Cosane-GO** turns out to be around 28 % less dispersible. This could be due to the different surfactant behaviour of $[B_{12}H_{12}]^{2-}$ *versus* cosane, as was previously reported by Teixidor and co.[12] This can account for better dispersibility of **B_{12}-GO** with respect to **cosane-GO**. Remarkably, after 1 month (Figure 4b) the water dispersibility of GO decreases in 33 % and both boron clusters modified-GO hybrid dispersions remain almost unaltered; **B_{12}-GO** shows about 32 % more dispersibility than GO and **Cosane-GO** preserves its degree of dispersibility, which now is slightly higher than GO. A picture of the analysed dispersions is included in the inset of Figure 4b. Noticeably, this indicates that the chemical modification of GO with these anionic boron clusters resulted in an improved stability of the aqueous dispersions. It becomes clear that covalent bonding of boron clusters onto graphene oxide changes the chemical-physical characteristics of the graphene surface. Thus, we have analysed as-prepared dispersions of the different materials in THF by UV-Vis and in acetone by visual inspection, due to its strong absorption below 340 nm. An evident increase of dispersibility was observed for THF dispersions of **Cosane-GO** hybrids respect to GO (Figure S12). In acetone (Figure S13), the GO dispersion is not stable[25] but the supernatant liquid of **Cosane-GO** and **B_{12}-GO** show noteworthy colour intensity after 1 hour. Consequently, these boron clusters play a crucial role on the dispersibility properties of the hybrid materials to markedly improve the stability of dispersions both in water and organic solvents. To the best of our knowledge, these are the first examples of boron modified-GO hybrids that show this feature, which is of great interest for further processing and applications.

To summarize, we have covalently grafted amine functionalized cosane and $[B_{12}H_{12}]^{2-}$ anions onto the surface of graphene oxide. The efficient covalent grafting was corroborated by FT-IR and XPS. TGA showed different weight loss for boron cluster compounds grafted onto graphene oxide compared to unmodified graphene, being the former more thermally stable. Remarkably, chemical modification of graphene oxide with these anionic boron clusters results in nanohybrids with an enhanced dipersibility both in water and in organic solvents as well as high stable aqueous dispersions, as assessed by UV-Vis. Notably, EFTEM imaging has provided elemental maps confirming the uniform distribution of the boron clusters on the graphene oxide flakes. In conclusion, the combination of cobaltabisdicarbollide and *closo*-dodecaborate anions with graphene oxide leads to new high boron content materials with exceptional physico-chemical and thermal properties. The development of applications for these nanohybrids is actually in progress.

Acknowledgements

This work has been supported by Ministerio de Economía y Competitividad, MINECO (CTQ2013-44670-R: MAT2014-53500-R) and Generalitat de Catalunya (2014/SGR/149). J.C.-G. thanks the CSIC for an Intramural grant. ICN2 acknowledges support from the Severo Ochoa Program (MINECO, Grant SEV-2013-0295).

Keywords: Graphene oxide • Dispersibility • Boron clusters• Electron Microscopy

[1] a) A. K. Geim, K. S. Novoselov, *Nat Mater* **2007**, *6*, 183-191; b) A. K. Geim, *Science* **2009**, *324*, 1530-1534; c) X. Huang, Z. Yin, S. Wu, X. Qi, Q. He, Q. Zhang, Q. Yan, F. Boey, H. Zhang, *Small* **2011**, *7*, 1876-1902.
[2] P. Wick, A. E. Louw-Gaume, M. Kucki, H. F. Krug, K. Kostarelos, B. Fadeel, K. A. Dawson, A. Salvati, E. Vázquez, L. Ballerini, M. Tretiach, F. Benfenati, E. Flahaut, L. Gauthier, M. Prato, A. Bianco, *Angew. Chem. Int. Ed.* **2014**, *53*, 7714-7718.
[3] a) D. Chen, H. Feng, J. Li, *Chem. Rev.* **2012**, *112*, 6027-6053; b) V. Georgakilas, M. Otyepka, A. B. Bourlinos, V. Chandra, N. Kim, K. C. Kemp, P. Hobza, R. Zboril, K. S. Kim, *Chem. Rev.* **2012**, *112*, 6156-6214; c) D. Bitounis, H. Ali-Boucetta, B. H. Hong, D.-H. Min, K. Kostarelos, *Adv. Mater.* **2013**, *25*, 2258-2268.
[4] a) C. J. Shearer, A. Cherevan, D. Eder, *Adv. Mater.* **2014**, *26*, 2295-2318; b) L. Cabana, B. Ballesteros, E. Batista, C. Magén, R. Arenal, J. Oró-Solé, R. Rurali, G. Tobias, *Adv. Mater.* **2014**, *26*, 2016-2021; c) L. Shao, X. Huang, D. Teschner, W. Zhang, *ACS Catal.* **2014**, *4*, 2369-2373.
[5] S. J. Kim, K. Choi, B. Lee, Y. Kim, B. H. Hong, *Annu. Rev. Mater. Res* **2015**, *45*, 63-84.
[6] a) C. Chung, Y.-K. Kim, D. Shin, S.-R. Ryoo, B. H. Hong, D.-H. Min, *Acc. Chem. Res.* **2013**, *46*, 2211-2224; b) K. Kostarelos, K. S. Novoselov, *Science* **2014**, *344*, 261-263; c) A. Servant, A. Bianco, M. Prato, K. Kostarelos, *Bioorg. Med. Chem. Lett.* **2014**, *24*, 1638-1649.
[7] a) R. N. Grimes, in *Carboranes (Second Edition)* (Ed.: R. N. Grimes), Academic Press, Oxford, **2011**, pp. 1053-1082; b) N. S. Hosmane, *Boron Science: New Technologies and Applications*, Taylor & Francis, **2011**; c) R. Kaplánek, P. Martásek, B. Grüner, S. Panda, J. Rak, B. S. S. Masters, V. Král, L. J. Roman, *J. Med. Chem.* **2012**, *55*, 9541-9548; d) M. Scholz, E. Hey-Hawkins, *Chem. Rev.* **2011**, *111*, 7035-7062.
[8] P. Matějíček, P. Cígler, A. B. Olejniczak, A. Andrysiak, B. Wojtczak, K. Procházka, Z. J. Lesnikowski, *Langmuir* **2008**, *24*, 2625-2630
[9] P. Bauduin, S. Prevost, P. Farràs, F. Teixidor, O. Diat, T. Zemb, *Angew. Chem. Int. Ed.* **2011**, *50*, 5298-5300.
[10] M. Tarrés, E. Canetta, C. Viñas, F. Teixidor, A. J. Harwood, *Chem. Commun.* **2014**, *50*, 3370-3372.
[11] K. B. Gona, A. Zaulet, V. Gómez-Vallejo, F. Teixidor, J. Llop, C. Viñas, *Chem. Commun.* **2014**, *50*, 11415-11417.
[12] C. Viñas, M. Tarrès, P. González-Cardoso, P. Farràs, P. Bauduin, F. Teixidor, *J. Chem. Soc., Dalton Trans.* **2014**, *43*, 5062-5068

[13] a) S. Tachikawa, T. Miyoshi, H. Koganei, M. E. El-Zaria, C. Viñas, M. Suzuki, K. Ono, H. Nakamura, *Chem. Commun.* **2014**, *50*, 12325-12328; b) M. Neumann, U. Kunz, H. Lehmann, D. Gabel, *J. Neuro-Oncol.* **2002**, *57*, 97-104.
[14] M. W. Lee, O. K. Farha, M. F. Hawthorne, C. H. Hansch, *Angew. Chem.* **2007**, *119*, 3078-3082.
[15] a) E. J. Juárez-Pérez, P. H. Mutin, M. Granier, F. Teixidor, R. Núñez, *Langmuir* **2010**, *26*, 12185-12189; b) E. J. Juárez-Pérez, M. Granier, C. Viñas, P. H. Mutin, R. Núñez, *Chem. - Asian J.* **2012**, *7*, 277-281; c) L. Cabana, A. González-Campo, X. Ke, G. Van Tendeloo, R. Núñez, G. Tobias, *Chem. Eur. J.* **2015**, *21*, 16792-16795.
[16] D. A. Morgan, J. Sloan, M. L. H. Green, *Chem. Commun.* **2002**, 2442-2443.
[17] A. Semioshkin, E. Nizhnik, I. Godovikov, Z. Starikova, V. Bregadze, *J. Organomet. Chem.* **2007**, *692*, 4020-4028.
[18] S. Sandoval, N. Kumar, A. Sundaresan, C. N. R. Rao, A. Fuertes, G. Tobias, *Chem. Eur. J.* **2014**, *20*, 11999-12003.
[19] V. Štengl, S. Bakardjieva, M. Bakardjiev, B. Štíbr, M. Kormunda, *Carbon* **2014**, *67*, 336-343.
[20] Y. Xue, Y. Liu, F. Lu, J. Qu, H. Chen, L. Dai, *J. Phys. Chem. Lett.* **2012**, *3*, 1607-1612.
[21] S. Niyogi, E. Bekyarova, M. E. Itkis, J. L. McWilliams, M. A. Hamon, R. C. Haddon, *J. Am. Chem. Soc.* **2006**, *128*, 7720-7721.
[22] A. González-Campo, B. Boury, F. Teixidor, R. Núñez, *Chem. Mater.* **2006**, *18*, 4344-4353.
[23] J. U. Kahlert, A. Rawal, J. M. Hook, L. M. Rendina, M. Choucair, *Chem. Commun.* **2014**, *50*, 11332-11334.
[24] S. Stankovich, D. A. Dikin, R. D. Piner, K. A. Kohlhaas, A. Kleinhammes, Y. Jia, Y. Wu, S. T. Nguyen, R. S. Ruoff, *Carbon* **2007**, *45*, 1558-1565.
[25] J. I. Paredes, S. Villar-Rodil, A. Martínez-Alonso, J. M. D. Tascón, *Langmuir* **2008**, *24*, 10560-10564.
[26] S. Sandoval, N. Kumar, J. Oro-Solé, A. Sundaresan, C. N. R. Rao, A. Fuertes, G. Tobias, *Carbon* **2016**, *96*, 594-602.
[27] R. Núñez, E. J. Juárez-Pérez, F. Teixidor, R. Santillan, N. Farfán, A. Abreu, R. Yépez, C. Viñas, *Inorg. Chem.* **2010**, *49*, 9993-10000